Spectral correlations of fractional Brownian motion

Tor Arne Øigård,[1] Alfred Hanssen,[1] and Louis L. Scharf[2]
[1]*Department of Physics and Technology, University of Tromsø, NO-9037 Tromsø, Norway*
[2]*Department of Electrical and Computer Engineering and Department of Statistics, Colorado State University, Fort Collins, Colorado 80523, USA*

(Received 13 March 2006; revised manuscript received 28 June 2006; published 14 September 2006)

Fractional Brownian motion (fBm) is a ubiquitous nonstationary model for many physical processes with power-law time-averaged spectra. In this paper, we exploit the nonstationarity to derive the full spectral correlation structure of fBm. Starting from the time-varying correlation function, we derive two different time-frequency spectral correlation functions (the ambiguity function and the Kirkwood-Rihaczek spectrum), and one dual-frequency spectral correlation function. The dual-frequency spectral correlation has a surprisingly simple structure, with spectral support on three discrete lines. The theoretical predictions are verified by spectrum estimates of Monte Carlo simulations and of a time series of earthquakes with a magnitude of 7 and higher.

DOI: 10.1103/PhysRevE.74.031114 PACS number(s): 05.40.Jc, 02.50.Ey, 05.45.Tp, 91.30.Px

I. INTRODUCTION

Fractional Brownian motion (fBm) is a useful nonstationary model for many fractal and long-range dependent processes of interest in physics, biology, finance, and telecommunications [1–3]. The characterization and understanding of such processes has become an important and surprisingly difficult problem [3]. A basic property of fBm is that its time-averaged power spectrum is proportional to $|\omega|^{-(2H+1)}$, where H is the Hurst parameter and ω is a frequency variable [1]. However, conventional power spectra only characterize stationary processes, so crucial spectral information about fBm's may be inaccessible through the standard description.

In this paper, we fully exploit the fact that fBm is a nonstationary random process. By evaluating the correlation structure in dual-frequency and time-frequency, we gain crucial insight about the second-order statistical properties of fBm. In particular, we show that the dual-frequency spectral correlation function has a surprisingly simple structure.

The time-frequency Wigner-Ville (WV) spectrum of fBm was derived and explored in Ref. [4]. However, the WV spectrum of fBm contains no distinct features, and it may be hard to interpret from a physical point of view. The time-dependent correlation function of fBm is well known [1,5,6] and this is a pure time-domain second-order characterization. As discussed in Refs. [7,8], the time-dependent correlation function is just one of four equivalent second-order characterizations of nonstationary processes. In this paper, we will systematically derive the three other second-order moment functions for fBm in closed form, and discuss their importance.

II. SPECTRAL CORRELATIONS

A useful time-domain formulation of a zero-mean fBm, $B_H(t)$, is given by [9–11]

$$B_H(t) - B_H(0) = \frac{1}{\Gamma(H+1/2)}\left[\int_{-\infty}^{0}[(t-s)^{H-1/2} - (-s)^{H-1/2}]dB(s) + \int_{0}^{t}(t-s)^{H-1/2}dB(s)\right]. \tag{1}$$

Here, $B(t)$ denotes standard zero-mean Brownian motion or a Wiener process, and $dB(t)$ is a differential increment of $B(t)$. The parameter $H \in (0,1)$ is the Hurst parameter and $\Gamma(\cdot)$ is the ordinary gamma function. Equation (1) generalizes ordinary Brownian motion, which is a special case of fBm with parameter $H=1/2$. The increments of fBm are statistically stationary and self-similar, i.e.,

$$B_H(t+a\tau) - B_H(t) \overset{d}{=} a^H B_H(\tau),$$

for any scale parameter $a>0$, and $t,\tau \in \mathbb{R}$ [4]. Here, $\overset{d}{=}$ denotes equality in distribution [12].

Our starting point is the dual-time temporal correlation function for fBm, $R_{B_H}(t,\tau)=\langle B_H(t)B_H(t+\tau)\rangle$, which evaluates to [5]

$$R_{B_H}(t,\tau) = \frac{V_H}{2}(|t|^{2H} + |t-\tau|^{2H} - |\tau|^{2H}), \tag{2}$$

where

$$V_H = \Gamma(1-2H)\frac{\cos(\pi H)}{\pi H}.$$

Here, $\langle\cdot\rangle$ denotes ensemble average, t is a *global* time variable, and τ is a *local* time variable. Since the process $B_H(t)$ is a zero-mean Gaussian process, it is uniquely characterized by a correlation function on the form of Eq. (2) [6]. The dual-time correlation function $R_{B_H}(t,\tau)$ represents but one way of expressing the nonstationary structure of fBm to second order.

A useful spectral representation of $B_H(t)$ is

$$B_H(t) = \int_{-\infty}^{\infty} e^{j\omega t} dZ(\omega), \tag{3}$$

where $dZ(\omega)$ is the complex-valued, nonorthogonal, infinitesimal stochastic Fourier generator for fBm, and $j=\sqrt{-1}$ is the imaginary unit. The dual-frequency spectral correlation of $dZ(\omega)$ is

$$\langle dZ(\omega) dZ^*(\omega-\nu)\rangle = S_{B_H}(\nu,\omega) d\omega d\nu/(2\pi)^2. \tag{4}$$

Here, ω and ν are global and local angular frequencies, respectively. The process $dZ(\omega)$ is a random set function that assigns complex random variables to frequency intervals [6]. The spectral correlation density function $S_{B_H}(\nu,\omega)$ is often called the dual-frequency spectrum, or the Loéve spectrum, and this is the quantity of primary interest in this paper.

The dual-frequency spectral correlation function describes the essential feature of nonstationary random processes, namely, that there is a correlation between the different frequency components [6,7]. Conversely, a stationary random process would have $S_{B_H}(\nu,\omega)=S_0(\omega)\delta(\omega-\nu)$ for some nonnegative function $S_0(\omega)$, and $\delta(\omega)$ Dirac's delta function. The function $S_0(\omega)$ is the conventional power spectrum. Thus, it is clear that for a stationary random process, the power spectrum is a second-order statistical quantity that contains all relevant spectral information. However, for nonstationary random processes, the spectral behavior is in general much more complicated due to correlations between frequency pairs. Hence, the dual-frequency correlation function should be considered explicitly when analyzing nonstationary random processes. According to Eq. (3), we may think of $B_H(t)$ as a superposition of complex oscillations $\exp(j\omega t)$ with correlated complex infinitesimal random amplitudes $dZ(\omega)$ [6,7].

The dual-time correlation function $R_{B_H}(t,\tau)$ is the bivariate inverse Fourier transform of $S_{B_H}(\nu,\omega)$ [7],

$$R_{B_H}(t,\tau) = \int_{-\infty}^{\infty}\int_{-\infty}^{\infty} S_{B_H}(\nu,\omega) e^{j(\nu t+\omega\tau)} \frac{d\omega d\nu}{(2\pi)^2}. \tag{5}$$

By performing the two-dimensional Fourier transform of $R_{B_H}(t,\tau)$ with respect to t and τ, we readily obtain the dual-frequency spectral correlation of fBm as

$$S_{B_H}(\nu,\omega) = 2\pi[|\omega|^{-(2H+1)}\delta(\nu) - |\omega|^{-(2H+1)}\delta(\nu+\omega) - |\nu|^{-(2H+1)}\delta(\omega)]. \tag{6}$$

This is the primary result of this paper, and a result that bears comment. We see that the spectral correlation function is real valued and that it is represented as a line spectrum with spectral support on three discrete lines. For $\nu=0$ the spectrum resides on the stationary manifold, so the particular spectral correlation $S_{B_H}(0,\omega)d\omega=\langle|dZ(\omega)|^2\rangle\sim|\omega|^{-(2H+1)}$ is the conventional stationary (or average) power spectrum. Stationary random processes would have a contribution only along this line. However, if the process is nonstationary, the dual-frequency spectrum $S_{B_H}(\nu,\omega)$ will have nonzero contributions also outside the stationary manifold. For $\omega=0$, we obtain the spectral correlation $S_{B_H}(\nu,0)d\nu=\langle dZ(0)dZ^*(\nu)\rangle\sim|\nu|^{-(2H+1)}$, which is a correlation between the dc component of the Fourier generator with all other frequency components. For $\nu=-\omega\neq 0$ we obtain $S_{B_H}(-\omega,\omega)d\omega=\langle dZ(\omega)dZ^*(0)\rangle\sim|\omega|^{-(2H+1)}$, which is also a manifestation of the correlation between the dc component of the Fourier generator, and all other frequency components. Thus, we have two distinct lines in dual-frequency that have the same interpretation, namely, that the dc component of the Fourier generator is correlated with all other frequency components. Due to the uniqueness of the dual-time correlation function for fBm, it is clear that the dual-frequency spectrum in Eq. (6) is a necessary and sufficient condition for a Gaussian process to be fBm.

To complete the second-order description of fBm, we now proceed by evaluating the two possible time-frequency descriptions. The time-frequency ambiguity density spectrum (or simply, ambiguity function) $A_{B_H}(\nu,\tau)$ is obtained by Fourier transforming $R_{B_H}(t,\tau)$ with respect to t,

$$A_{B_H}(\nu,\tau) = 2\cos\left[\frac{\pi}{2}(1+\nu\tau)\right]|\nu|^{-2H+1}e^{-j\nu\tau/2} - \pi V_H|\tau|^{2H}\delta(\nu). \tag{7}$$

The ambiguity function is a function of local time τ and local frequency ν, and it is of great importance in echo-based sounding systems for the simultaneous estimation of time delay and Doppler shift.

The last second-order descriptor is the so-called time-frequency Kirkwood-Rihaczek (KR) spectrum [13,14] $P_{B_H}(t,\omega)$. This spectrum is obtained by Fourier transforming $R_{B_H}(t,\tau)$ with respect to the local time variable τ. It is easy to obtain the following KR spectrum for fBm:

$$P_{B_H}(t,\omega) = \pi V_H|t|^{2H}\delta(\omega) + 2\sin\left(\frac{\omega t}{2}\right)e^{-j(\omega t/2-\pi/2)}|\omega|^{-(2H+1)}. \tag{8}$$

We see that the KR spectrum $P_{B_H}(t,\omega)$ is a global time, global frequency representation of the second-order statistical properties of fBm. It is important to understand that the KR spectrum is in fact an *inner product* between the fBm process itself, $B_H(t)$, and the complex demodulated random Fourier generator [8]

$$\langle B_H(t) dZ(\omega) e^{j\omega t}\rangle = P_{B_H}(t,\omega) d\omega/2\pi. \tag{9}$$

By adapting the analysis for the WV spectrum presented in Ref. [4] to the present KR time-frequency spectrum, we gain interesting insight. If the time variable of fBm is scaled by $a>0$, then we can show the following associated scaling property for the KR time-frequency spectrum of fBm:

$$\frac{1}{a}P_{B_H}(at,\omega/a) = P_{a^H B_H}(t,\omega).$$

This result manifests a second-order self-similarity of fBm through the KR spectrum. If we define the average KR spectrum over a symmetrical time interval of length T,

$$P_{B_H}(\omega;T) = \frac{1}{T}\int_{-T/2}^{T/2} P_{B_H}(t,\omega)dt,$$

we in the limit $T\to\infty$ obtain

$$\lim_{T\to\infty} P_{B_H}(\omega;T) \sim \frac{1}{|\omega|^{2H+1}}, \quad \omega \neq 0.$$

This is the well-known conventional time-averaged power spectrum of fBm (e.g., Ref. [4]).

The relation between the four second-order moment functions we have derived, can be summarized by the following diagram:

$$\begin{array}{ccc} R_{B_H}(t,\tau) & \overset{\tau\leftrightarrow\omega}{\longleftrightarrow} & P_{B_H}(t,\omega) \\ t\leftrightarrow\nu \updownarrow & & \updownarrow t\leftrightarrow\nu \\ A_{B_H}(\nu,\tau) & \underset{\tau\leftrightarrow\omega}{\longleftrightarrow} & S_{B_H}(\nu,\omega) \end{array} \tag{10}$$

In Eq. (10), adjacent corners in the diagram are within one Fourier transform from each other, while opposite corners are within two Fourier transforms from each other. The variables involved in the transformations are indicated in the diagram. Any one of the four basic quantities $R_{B_H}(t,\tau)$, $P_{B_H}(t,\omega)$, $A_{B_H}(\nu,\tau)$, and $S_{B_H}(\nu,\omega)$ characterize the complete second-order statistics of fBm. Note that while $R_{B_H}(t,\tau)$, $P_{B_H}(t,\omega)$, and $S_{B_H}(\nu,\omega)$ are inner products, $A_{B_H}(\nu,\tau)$ is not.

III. CASE STUDIES

To verify the theoretical prediction that the dual-frequency spectral correlation of fBm has its spectral support on three discrete lines, we conducted relevant Monte Carlo simulations and analyzed a time series of global seismic activity.

A. Synthetic fBm

We synthetically generated a fBm time series of length $N=512$ by means of the synthesizer in Ref. [15]. To estimate the dual-frequency spectrum we applied the state-of-the-art nonparametric multitaper approach introduced by Ref. [16]. The method is based on the application of orthogonal data tapers (the discrete prolate spheroidal sequences), which maximize the energy concentration in the frequency band $(-B,B)$ and average over a set of spectral estimates. The *time-bandwidth product NB* is an important parameter which controls the degree of smoothing [16] along the stationary manifold in the frequency domain. In our simulations the time-bandwidth product was chosen to be $NB=3.5$, as this value provided a good compromise between resolution and smoothing. The estimate was obtained through $M=1000$ Monte Carlo simulations.

In Fig. 1 we show the mean value of the modulus of the estimated spectral correlation $\hat{S}_{B_H}(\nu,\omega)$ from a synthetic fBm process with $H=0.1$. We observe that the predicted vertical, horizontal, and diagonal lines of support are clearly present.

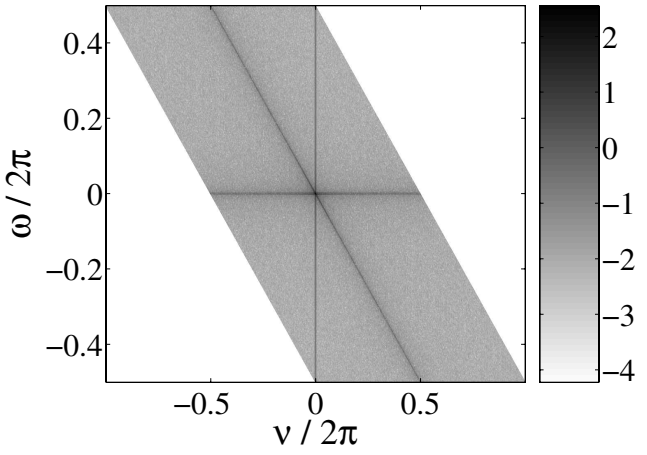

FIG. 1. Logarithm of the modulus of estimated spectral correlation, based on synthetic fBm data with $H=0.1$.

The stationary manifold, i.e., $\nu=0$, will always be present. From Fig. 1 we see also that the two predicted distinct lines outside the stationary manifold are distinctly visible as predicted. These lines are a direct manifestation of the spectral correlation structure specific for fBm, and they provide us with a surprisingly simple characteristic signature for the complex nonstationarity involved.

Numerical simulations show that detailed estimation of the dual-frequency spectrum for fBm may be a difficult task. Both the skewness and the variance outside the stationary manifold increase with increasing H, due to spectral leakage out from the spectral peak. In Fig. 2 we show the empirical standard deviation of the dual-frequency spectrum. We see that the estimation error is larger for the lines of spectral support outside the stationary manifold. Numerical simulations show that the estimation error an increases with increasing value of H and with a decreasing size of the data set. However, even though the details along the lines of support may be imprecise, the important feature is that the mere presence of these lines is an important manifestation of fBm.

In Fig. 3 we show the estimated dual-frequency correlation of a low sized synthetic fBm data set. The data set

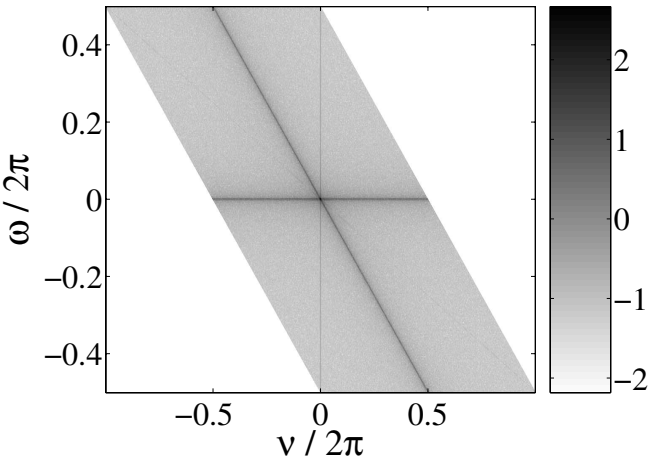

FIG. 2. Logarithm of the empirical standard deviation of the spectral correlation for synthetic fBm data with $H=0.1$.

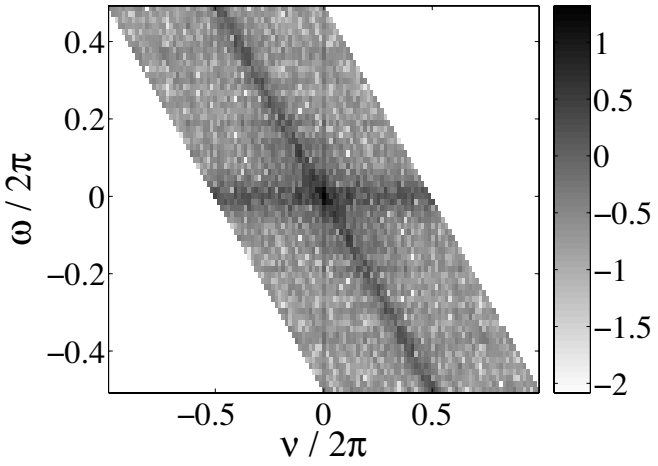

FIG. 3. Logarithm of the modulus of the estimated spectral correlation for a single realization of synthetic fBm of length $N=128$ and with $H=0.1$.

consists of a single realization of a time series of length $N=128$ samples. Several properties of the estimator are easily identified from Fig. 3. We see that the lines of support outside the stationary manifold are much wider and has a greater intensity than the stationary manifold. This is due to the smoothing and variance properties of the estimator.

In Fig. 4 we show the detailed behavior of the estimated dual-frequency correlation on the stationary manifold $\nu=0$ (full line), and on the diagonal $\omega=-\nu$ (dashed line). The power-law behavior is evident in both cases, and the variability of the dashed line is a manifestation of the larger variance outside the stationary manifold. The tendency for both curves to flatten towards the highest frequencies is an effect of bias due to spectral leakage. For processes with power-law spectra, the leakage-induced bias is more pronounced at high frequencies than at low frequencies.

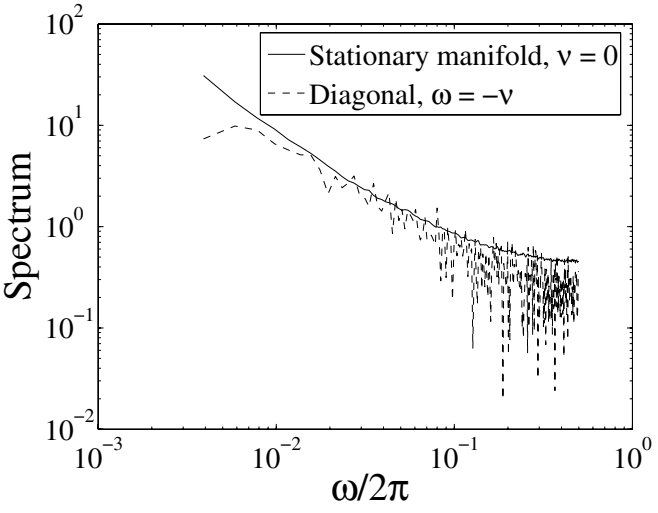

FIG. 4. Logarithm $(10\log_{10})$ of the modulus of the estimated spectral correlations on the stationary manifold, $\nu=0$ (full curve), and on the diagonal, $\omega=-\nu$ (dashed curve), for synthetic fBm data with $H=0.1$.

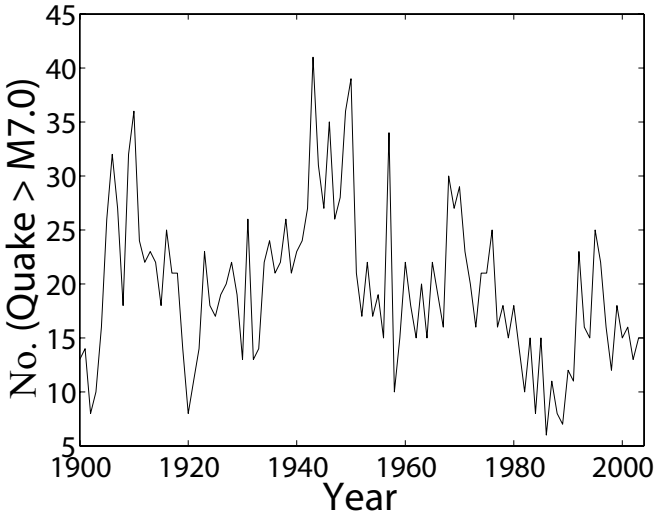

FIG. 5. The number of earthquakes with a magnitude greater than 7.0 on Richter's scale from 1900 to 2004.

B. Seismic activity

As a demonstration and application to interesting real world data, we have analyzed a times series containing the number of earthquakes with magnitude greater than 7.0 on Richter's scale. The time series contains data for every year since 1900 up to 2004, giving it a total of $N=105$ measurements. In Fig. 5 we show the time series, which has been obtained from the Earthquake Data Base System of the U.S. Geological Survey, National Earthquake Information Center.

In Fig. 6 we display the modulus of the estimated dual-frequency spectral correlation for the earthquake data set. The time-bandwith product for the estimator was chosen to be $NB=1.5$. Our analysis shows that these data indeed have a dual-frequency spectral correlation structure that is characteristic of fBm, with three distinct lines of support. The stationary manifold $\nu=0$ is present, but hard to discern. This is due to the small data set and the statistical properties of the

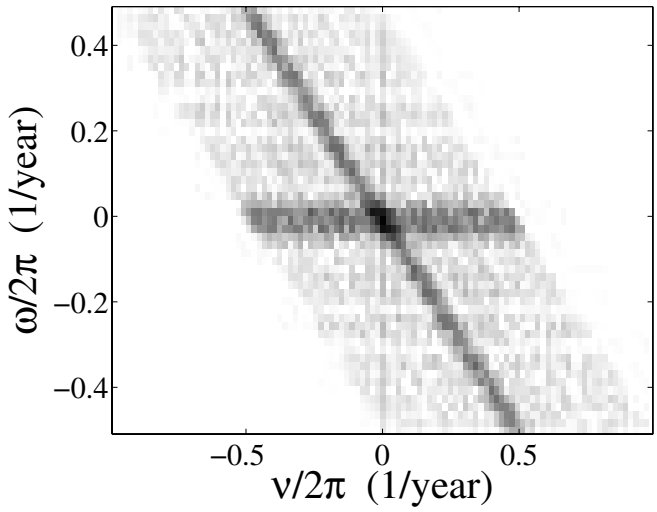

FIG. 6. Logarithm $(10\log_{10})$ of the modulus of the estimated spectral correlation for the earthquake data set.

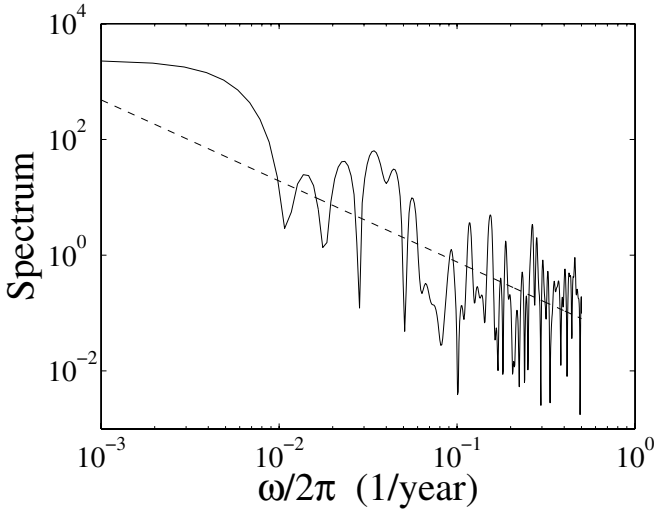

FIG. 7. Logarithm ($10\log_{10}$) of the estimated spectral correlations on the stationary manifold for the earthquake data. Dashed line: linear least-squares fit.

estimator. Also, since the estimator only smooths along the ω axis the lines of spectral support outside the stationary manifold will appear wider than the stationary manifold.

It is natural to question the result of the analysis of the seismic activity since the amount of data is very small. However, we believe that the fact that we are able to see the three spectral lines of support from such a small data set actually strengthens the result. The actual values on the spectral lines of support cannot be trusted, but the mere dual-frequency correlation structure that we predict in Eq. (6) is present. In fact, the result is highly comparative with the dual-frequency spectrum estimate from a small synthetic fBm data set shown in Fig. 3.

In Fig. 7 we show the estimate of the stationary manifold of the dual-frequency spectrum. This spectrum confirms that a power-law behavior is evident, and the overlaid dashed line corresponds to a Hurst parameter of $H=0.2$.

It is very interesting that the time series of strong earthquakes clearly exhibits dual-frequency characteristics of fractional Brownian motion. At present, we are not in a position to offer a physical explanation for this scale-invariance property of the time series. Note, however, that sliding fractional Brownian fault profiles has been proposed as a source of several observed features of earthquakes [17]. It was recently shown in Ref. [18] that certain pulse-train generator systems with threshold-controlled stochastic dynamics form a Brownian time series of a similar kind. Also, it has recently been shown in Ref. [19] that a time series of the waiting times between earthquakes is long range temporally correlated, and that this indicates that earthquake occurrences may depend on the geological history of a vast region. We believe that the frequency correlation structure of fBm that we predict, and the associated frequency correlations we have observed for earthquake data, may prove to be important information for understanding earthquake dynamics.

IV. CONCLUSION

In this paper we derived the complete second-order statistical correlation structure of fBm. By the use of the well-known dual-time correlation function we derived two different time-frequency spectral correlation functions, i.e., the ambiguity function and the Kirkwood-Rihaczek spectrum, and the dual-frequency spectral correlation function. The main result in this paper is the dual-frequency spectral correlation function. This is due to its surprisingly simple structure, with spectral support confined on three discrete lines, and the physical implications of these lines. The transformation from the time-domain correlation function to the spectral-domain correlation function provides us with a measure where the nonstationary behavior of fBm is more illuminating. We now interpret the nonstationary behavior of fBm to be caused by the correlation between the dc component of the infinitesimal Fourier generator and all other frequencies of the infinitesimal Fourier generator. Thus, we believe that this is an important quantity for characterizing fBm. The theoretical predictions were verified by both Monte Carlo simulations of synthetic fBm and real seismic activity data. Due to the uniqueness of the dual-frequency spectrum, one might formulate tests on whether a given data set has the same spectral-correlation structure to that of fBm.

ACKNOWLEDGMENTS

T.A.Ø. thanks the Fulbright Foundation of Educational Exchange, A.H. thanks the Research Council of Norway, and L.L.S. thanks the U.S. Office of Naval Research for its continued support.

[1] B. B. Mandelbrot, *The Fractal Geometry of Nature* (Freeman and Co., New York, 1982).
[2] *Fractals in Physics*, edited by L. Pietronero and E. Toscatti (North-Holland, Amsterdam, 1986).
[3] R. F. Voss, Phys. Rev. Lett. **68**, 3805 (1992).
[4] P. Flandrin, IEEE Trans. Inf. Theory **35**, 197 (1989).
[5] A. N. Kolmogorov, Compt. Rend. **26**, 943 (1940).
[6] A. M. Yaglom, *Correlation Theory of Stationary and Related Random Functions I—Basic Results* (Springer-Verlag, New-York, 1987).
[7] A. Hanssen and L. L. Scharf, IEEE Trans. Signal Process. **51**, 1243 (2003).
[8] L. L. Scharf, P. Schreier, and A. Hanssen, IEEE Signal Process. Lett. **12**, 297 (2005).
[9] B. B. Mandelbrot and J. W. V. Ness, SIAM Rev. **10**, 422 (1968).
[10] I. S. Reed, P. C. Lee, and T. K. Truong, IEEE Trans. Inf. Theory **41**, 439 (1995).
[11] G. Samorodnitsky and M. Taqqu, *Stable Non-Gaussian Random Processes, Stochastic Models with Infinite Variance* (Chapman & Hall, London, 1994).
[12] M. S. Taqqu, in *Theory and Applications of Long-Range De-*

pendence, edited by P. Doukhan, G. Oppenheim, and M. S. Taqqu (Birkhäuser, New York, 2003).
[13] G. Kirkwood, Phys. Rev. **44**, 31 (1933).
[14] A. Rihaczek, IEEE Trans. Inf. Theory **14**, 369 (1968).
[15] S. B. Lowen, Methodol. Comput. Appl. Probab. **1**, 445 (1999).
[16] D. J. Thomson, Proc. IEEE **70**, 1055 (1982).
[17] V. De Rubeis, R. Hallgass, V. Loreto, G. Paladin, L. Pietronero, and P. Tosi, Phys. Rev. Lett. **76**, 2599 (1996).
[18] J. Davidsen and H. G. Schuster, Phys. Rev. E **65**, 026120 (2002).
[19] N. Scafetta and B. J. West, Phys. Rev. Lett. **92**, 138501 (2004).